

Thermodynamics of polyamorphism ポリアモルフィズムの熱力学

Kazuhiro Fuchizaki
渚崎 員弘

Department of Mathematics, Physics and Earth sciences, Graduate School of Science and Engineering, Ehime University, 2-5 Bunkyo-cho, Matsuyama, 790-8577, Japan
愛媛大学大学院理工学研究科数理物質科学専攻

Abstract

A substance in a solid state can take more than a crystalline phase. For example, ice, a solid form of water, has nineteen crystalline phases. Each solid state has a different structure because water molecules are located on discrete lattice points with different symmetry. Then, the problem is whether a liquid state without a long-range order can take more than a single phase. Water has been considered to have two forms; one is low density and the other high density. The problem is named polyamorphism because of the involvement of polyamorphs. An occurrence of polyamorphism has been pointed out on a thermodynamic basis. At the beginning of this century, experimental evidence of polyamorphism was given for liquid phosphorus. This exciting experimental finding has revived the old theory of polyamorphism and activated the hunting of substances exhibiting polyamorphism. This review picks up essential substances stimulating the subsequent theoretical development. Therefore, the author also explains the original and recent theories in some detail. We have now attained a consensus regarding water polyamorphism through the theories. The author also mentions the crucial problems that remain unanswered.

Key Words: Polyamorphism, Liquid–liquid transition, Ginzburg–Landau form

1 Introduction

This century has begun with great excitement among scientists studying structural phase transitions in noncrystalline substances; two thermodynamically stable liquid phases were observed *in situ* in liquid phosphorus (Katayama et al. (2000)). They were shown to coexist, evidencing a discontinuous transition between the two liquids (Katayama et al. (2004)). An occurrence of a phase transition in liquids was suggested quite a long time ago on a theoretical basis, and candidates have been suggested (Rapoport (1967)). The rigorous evidence opened up an entrance to the thermodynamics of polyamorphism. This article reviews how we have described the phenomena and tried to extend the description. The author will mention the current status of the recent theoretical formulation.

Before proceeding further, it needs to explain the word “polyamorphism” because it seems still uncommon other than the relevant scientific communities. Some substances may have more than a phase in condensed states, even consisting of a single com-

ponent. Typical examples are allotropes of sulfur, carbon, oxygen, and phosphorus. For example, a match that used to be made of yellow-white phosphorus uses red phosphorus. The thermodynamically stable form of an expensive diamond at ambient conditions is graphite used in pencil. Such a substance with more than one crystalline state exhibits polymorphism. When a substance has some non-crystalline states, i.e., polyamorphic states, it shows polyamorphism. In the beginning, the polyamorphic states, i.e., polyamorphs, were restricted to amorphous states. Currently, they include not only solid but also liquid states (McMillan et al. (2007)).

There is a crucial substance that is inevitable in defining polyamorphism. The substance is water, which is fundamental in every living thing and global environment. The solid state of water, i.e., ice, consists of nineteen phases depending on pressure and temperature accessible to us (Yamane et al. (2021)). That is, water shows polymorphism. Mishima noted a negative Clapeyron slope of ice I_h 's melting curve; the melting point of ice I_h decreases with pressure. When compressed across the melting curve, he expected ice

I_h to “melt” retaining a solid state. He thus found amorphous ice (Mishima et al. (1984)), which transformed discontinuously to lower-density amorphous ice upon decompression (Mishima et al. (1985)). The observation provided evidence that ice has (at least) two amorphous states with different densities separated by a boundary, which was the first example of an apparently first-order transition between amorphous solids. This experimental demonstration of the existence of multiple *noncrystalline* states has made the word polyamorphism gradually prevalent in condensed matter physics, chemistry, materials, and Earth science.

The two amorphous ice states’ findings offered indirect evidence of two water phases with different densities, although the waters would never be real entities (Angell (2004)). However, to answer whether water can exist as two different (metastable) states (Gallo et al. (2016)) is crucially essential to understand why pieces of ice can float in water physically. (A solid-state substance usually has a higher density than its liquid counterpart.) Thermodynamic treatments for polyamorphs naturally were then extended to involve liquid states as well, and we now use polyamorphism both for amorphous and liquid states. In particular, many theoretical trials to understand the thermodynamic anomalies exhibited by water have developed the thermodynamics of polyamorphism. Water thus offers fertile ground in understanding the concept and guiding the theoretical development of polyamorphism, and water’s polyamorphism is explained in the next section in some detail.

This review begins with summarizing substances whose polyamorphism was indispensable to developing theories. Here, we focus on liquid–liquid transitions (LLTs), in which thermodynamically stable states, i.e., liquid phases, are involved in the transitions because metastable states such as amorphous states themselves are too subtle in describing the transitions. Although considerable numbers of substances have been reported since the first unambiguous identification for liquid phosphorus, most are metastable liquid states with a relatively short lifetime, or even candidates not observed (*in situ*). Therefore, in this review, the author restricts to mention the substances with thermodynamically stable liquid phases, the only exception being water.

The third section introduces the pioneering work, which served as a landmark for investigating polyamorphism, followed by the primary theoretical treatments. Through these theories, we currently achieve a consensus on water polyamorphism.

The final section concludes the article by pointing out significant challenges for the future.

2 Key Substances

The first clear identification of an LLT for liquid phosphorus achieved by Katayama et al. (Katayama et al. (2000)) stimulated experimental research. Large-scale hunting of substances and materials exhibiting an LLT has thus started. Meanwhile, theoretical research has conducted large-scale computations using first-principles calculations and simulations to explain or predict the LLT.

The guiding principle for the hunt was a melting anomaly typified by a melting maximum (Rapoport (1967)), which will be explained in the third section. Indeed, early studies have relied on this concept. Liquid polyamorphism emerges at extreme conditions such as at high pressure. This restriction is still too severe to measure an LLT *in situ*, especially the changes in structure and density upon an LLT. Therefore, early studies tried to detect an LLT from a subtle jump in *in situ* electrical resistance measurements under high pressure and temperatures. Researchers have become capable of conducting direct diffraction and absorption measurements using synchrotron x-ray sources with very high energy and low emittance developed in this century.

The introduction mentions that water has a melting curve with a negative Clapeyron slope. Yttria-alumina compound also has a negative-slope melting curve at higher temperatures such as 1800 K at ambient pressure (McMillan et al. (2003)). A tricky experimental technique called the aerodynamic levitation technique, combined with synchrotron x-ray spectroscopy, was applied to measure *in situ* the first-order LLT (although the result was controversial) (Greaves et al. (2008)). Researchers thus tried to flock into leading groups, making high-impact scientific journals cover.

Many substances are claimed to show liquid polyamorphism today, but most of them are in metastable states. A nearly complete list of the substances is available in a recent review (Tanaka (2020)). This article touches on a few substances showing polyamorphism between thermodynamically stable liquids. The author intends to present not a complete list but the substances that develop the theory.

Although the bonding nature of those substances with polyamorphism varies widely, they have one characteristic in common: two kinds of “species,” which sometimes might be different local orders with

different densities. Though not precisely identified, the species are explained in the following examples.

2.1 Water

We had still not been able to give clear-cut answers for the origin of the thermodynamic anomalies of water (Angell (2004)). However, the understanding has been appreciably promoted in the last decade to clarify the whole aspect of water polyamorphism. The critical hint is that all of the isothermal compressibility, isobaric heat capacity, and isobaric expansivity seem to diverge toward $-45\text{ }^{\circ}\text{C}$. Quite ingenious scenarios such as singularity-free (Sastry et al. (1996)) and critical-point free (Angell (2008)) scenarios were invented to explain the observed anomalies. The anomalies above remind us of the singularity appearing within a neighborhood of a critical point (Poole et al. (1992)). Indeed, we can explicate water’s anomalies simply but consistently by assuming that the singular point is a critical point between two liquid phases, the hypothesized thermodynamically stable states for the amorphous ices mentioned in the Introduction. The recent theories converge to support this critical-point scenario, which is referred to in the next section.

The two kinds of “species” for water might be two alternative forms of molecular arrangements giving different densities, i.e., a low-density liquid (LDL) and high-density liquid (HDL) corresponding to low-density amorphous (LDA) and high-density amorphous (HDA) ices. Unfortunately, the hypothesized critical point lies below the kinetic limit of homogenous ice formation, i.e., in the no man’s land (Mishima & Stanley (1998)) (see Fig. 1 of Fuchizaki (2016)). Hence, we cannot directly observe the two liquids. Tricky trials such as confining a water droplet within a nanosize region to pull up the critical point outside the no man’s land have been made to confirm the validity of the critical-point scenario (Holten et al. (2012)).

2.2 Tellurium

In conjunction with polyamorphism of water, it is worth mentioning polyamorphism of tellurium, although its emergence was successfully detected in the supercooled region in the last century (Tsuchiya (1991)). That is, the twofold liquid of tellurium, albeit a metastable state, lies outside no man’s land.

Liquid tellurium undergoes a gradual semimetal-metal transition with increasing temperature (Menelle et al. (1987)). This transition has been associated with a structural evolution accompanying a density increase in the liquid phase. The two

“species,” in this case, are called the L-form and H-form of atoms with higher coordination numbers compared to the former ones. Because the melting point, $450\text{ }^{\circ}\text{C}$, was believed to be already at the lower boundary of the H-form, the liquid was supercooled more than 100 degrees below the melting point by making the sample size reduced to 0.6 cm in length \times 0.34 mm in diameter. The extrema in the excess specific heat, isothermal compressibility, and isobaric thermal expansion coefficient, evidencing the transition between the L-form and H-form dominant liquids, were confirmed. These thermodynamic anomalies were quantitatively rationalized by a kind of pseudobinary regular solution model mentioned in the next section, considering the concentration of H-form atoms.

2.3 Hydrogen

Solid molecular hydrogen was predicted to transform to atomic metallic hydrogen almost a hundred years ago (Wigner & Huntington (1935)). Since then, theorists and experimentalists have tried to prove the existence of metallic hydrogen.

Ab initio calculations predicted the melting curve of solid H_2 with a maximum at about 90 GPa and 1000 K (Bonev et al. (2004)), which was confirmed by experiments (Deemyad & Silvera (2008)). A discontinuous LLT from molecular to atomic metallic hydrogen, named the plasma phase transition, was then anticipated. The LLT is also an insulator-metal transition. Zaghoo et al. insisted that they could capture the transition from their transmittance and reflectance measurements by heating a sample to 2200 K at 170 GPa using pulsed laser heating and a DAC (Zaghoo et al. (2016)). The sharp increase (decrease) in reflectivity (transmissivity) and the plateaus in the heating curves, explained as arising from latent heat, might indicate a discontinuous nature of the transition. The phase line was found to have a negative slope. However, the measuring pressure was too high to detect the liquid-liquid critical point (LLCP). Refer to Fig. 1 of Zaghoo et al. (2016) for the polyamorphic phase diagram, including their result of measurements and other experimental and theoretical outcomes.

The two “species,” in this case, are the two forms of hydrogen: molecular, nonmetallic, and atomic, metallic.

2.4 Cerium

Cadien et al. observed a transition from a high-density to a low-density liquid phase of cerium through *in situ* x-ray diffraction measurements us-

ing a DAC and laser heating (Cadien et al. (2013)). A density decrease of 14% accompanied the transition upon heating from 1550 to 1900 K at 13 GPa. They also conducted the *ab initio* calculations using VASP package (Kresse & Hafner (1994)) to extract the twofold valence states, Ce^{f_0} (trivalent) and Ce^{f_1} (tetravalent), to account for the measured structures. Thus, the “species” are Ce atoms with those valence states caused by the delocalization of 4f electrons.

Identification of the two species allowed them to construct a pseudobinary regular solution model, from which they concluded that the discontinuous LLT would terminate at 21.3 GPa and 2100 K, the LLC. Figure 4 of Cadien et al. (2013) summarizes the expected polyamorphic behavior as the phase diagram.

2.5 Silicon

The validity of the critical-point scenario for an LLT of water has remained unanswered because the hypothesized critical point is located deep in the no man’s land. It is then natural to look for another substance with a similar structure to address the issue. The structure in question is known as an open tetrahedrally network structure.

Crystalline silicon, c-Si, belonging to the class of tetrahedral systems, is expected to have the LLC at 1100 K and -1 GPa (McMillan et al. (2005)). Beye et al. instantaneously heated c-Si by supplying ultrashort optical pulses of femtosecond duration to excite the valence electrons near the edge (Beye et al. (2010)). The energy supplied was transferred to the nuclear system, destroying the short-range order with the sample density unchanged. c-Si was thus brought into a metastable LDL state. The latent heat for this change was then transferred to the atomic structure, which was “melted” into an HDL state. They measured the electronic-structure evolution as a function of pump-probe delay and concluded the occurrence of the two-step transition from the semiconducting c-Si with the bandgap through the semimetallic LDL state with a pseudogap to the metallic HDL state without a gap. The second (liquid–liquid) transition seems discontinuous because the energetic structure changes are quite abrupt compared to the smooth decay of electrons in the conduction band. As the driving force behind the second transition, they insisted on the densification upon melting, which should be shared with the tetrahedral systems.

Therefore, the two “species” regarding the transition are two alternative condensed amorphous states caused by the excitation of electrons near the edge.

2.6 Phosphorus

Probably, phosphorus and sulfur (mentioned below) may be the only substances that have been widely accepted as the substances undergoing a transition between the two thermodynamically stable liquid phases.

Like water and silicon, black phosphorus is also a member of the tetrahedral systems. Like SnI_4 (see below), its melting curve has a positive slope but is abruptly bent at about 1 GPa and 900 K (Akahama et al. (1987)). The slope above 1 GPa is smaller than below 1 GPa. The phase transition boundary seems to emanate from the kink point with a negative slope. (For the phase diagram, see Fig. 1 of Katayama et al. (2000), in which the melting line was drawn to have a maximum. A version with the maximum redrawn as a sharp corner has not been published.) The LLC, the endpoint of the boundary, was proposed at about 3500 K and 0.02 GPa (Zhao et al. (2017)). The LDL phase on the lower pressure side of the boundary is a molecular liquid consisting of P_4 molecules, whereas the HDL phase on the right is a polymerized liquid. The density difference between the LDL and HDL phases amounts to about 1.0 g/cc (Katayama et al. (2004)). Molecular and polymerized phosphorus atoms thus constitute the two “species.” Surprisingly, Katayama et al. succeeded in taking a snapshot of the coexistent states of LDL and HDL using x-ray radiography (Katayama et al. (2004)), supporting that the transition is of the first order.

2.7 Sulfur

To the best of the author’s knowledge, sulfur may be the only substance whose polyamorphism regarding the LLT is vividly unveiled by *in situ* x-ray diffraction, absorption, and Raman scattering measurements (Henry et al. (2020)). The polyamorphic phase diagram of sulfur is shown in Fig. 1 below. The phase boundaries and the LLC are indicated based on the actual measurements without any aid from theoretical and computational means.

The LLT of sulfur has been controversial because of the known λ -transition at a low-pressure region near atmospheric pressure (Sauer & Borst (1967)). The low-pressure liquid state constitutes molecules even experiencing the λ -transition. S_8 molecules, the constituents of crystalline α -S, are opened up at temperatures above the λ -transition to form polymeric chains or rings. The fraction of polymerization is 60% at most, even at the boiling point.

Upon compression along an isotherm below the critical-point temperature, the molecular liquid trans-

forms to a purely polymeric liquid consisting of long S chains concomitant with a sudden increase of density. As in the case of phosphorus, the coexistence of the two liquid phases was captured by x-ray radiography. However, unlike phosphorus (and water, though putatively), the liquid–liquid phase boundary has a positive Clapeyron slope. Although this feature shares with that of an ordinary liquid–gas phase boundary, the temperature dependence of the density difference is conclusively different; the density difference monotonically increases with lowering temperature along a gas–liquid coexistence line, whereas it decreases through a maximum in sulfur. Henry et al. speculated that entropy rather than density governs sulfur’s LLT (Henry et al. (2020)). The accessibility near the critical point located at about 1000 K and 2.2 GPa will facilitate us to inquire about the essential thermodynamics of an LLT.

Two “species” for the LLT are molecular and polymerized forms of S atoms.

2.8 Tin tetraiodide

We have discussed simple substances thus far except water. Here, we focus on SnI_4 , one of the compounds whose polyamorphic nature has been extensively studied.

SnI_4 has been known to undergo pressure-induced solid-state amorphization (SSA) at ~ 15 GPa under room temperature (Fujii et al. (1985)). As explained in the Introduction, amorphization may be the melting of a crystalline state within a solid-state field by crossing the metastable extension of a melting curve. SnI_4 was thus considered one of the substances undergoing SSA with a melting anomaly (Fuchizaki et al. (2000)).

Like water, the amorphous state transforms to another amorphous state with a lower density (Hamaya et al. (1997)). The originally discovered amorphous state, called Am-I, is formed due to molecular dissociation, whereas the lower-density amorphous state, Am-II, consists of irregularly oriented SnI_4 molecules. The transformation was found to be reversible. The existing limit of Am-I and Am-II were identified to be 3 and 7 GPa at room temperature, respectively. A recent reverse Monte Carlo analysis for the synchrotron x-ray diffraction data up to 30 GPa proposed the existence of another amorphous state, Am-III, which is transformed from Am-I at around 18 GPa on compression (Fuchizaki et al. (2021)). See Appendix A for the reverse Monte Carlo analysis. According to the analysis, partially dissociated molecules are connected to metallic I_2 bonds penetrated throughout

the system, whereas molecules are entirely dissociated in Am-III. No discontinuous change in density is expected upon the transition between Am-I and Am-III.

Against our anticipation, *in situ* measurements utilizing synchrotron x-ray diffraction revealed that the melting curve has a positive Clapeyron slope with a break at about 1.5 GPa and 1000 K, beyond which the slope becomes almost flat against pressure (Fuchizaki et al. (2004)). The liquid structure below and above the breakpoint differs (Fuchizaki et al. (2009)). The low-pressure liquid, called Liq-II, was identified as a molecular liquid consisting of SnI_4 molecules with perfect tetrahedral symmetry. In contrast, the high-pressure liquid, Liq-I, contains heavily deformed molecules with point symmetry C_{3v} (Fuchizaki et al. (2019)). It is highly expected that the metastable state of Liq-II (Liq-I) corresponds to Am-II (Am-I).

Furthermore, *in situ* synchrotron x-ray absorption measurement discovered a slight but nontrivial density difference of ~ 0.4 g/cc between the two liquids (Fuchizaki et al. (2013)). The absorption measurements upon compression along isotherms detected a density jump below 1000 K, above which a density variation became continuous. The fact indicates the LLCP at ~ 1000 K and 1.5 GPa, as predicted from the pseudobinary regular solution model (Fuchizaki et al. (2011)). Two different orientations between adjacent molecules were responsible for the two “species” in constructing the model. The model also assumed that the breakpoint on the melting curve is the triple point among Liq-II, Liq-I, and the crystalline phases.

The pseudobinary regular solution model thus consistently explains the whole polyamorphism observed thus far (Fuchizaki et al. (2011)). SnI_4 exhibits the water-type polyamorphism but with the LLCP accessible to us. Figure 3 of Fuchizaki (2016) depicted the polyamorphic aspect below 6 GPa in the phase diagram together with the two typical molecular orientations. “The pressure-induced SSA turned out to be only the ‘tip of the iceberg’ of the phenomena (Fuchizaki et al. (2021)).”

2.9 Melting anomaly and a slope of the liquid–liquid phase boundary

Figure 1 shows the phase diagram of sulfur. The author redraws to display it among the substances explained above because the liquid–liquid phase boundary was investigated by purely experimental observations for a bulk of sulfur. The measuring pressure and temperature were determined adequately within the

Table 1 The aspect of melting anomaly (the first row designated as “anomaly”) and the slope’s sign of the liquid–liquid boundary (the second row, “slope”) of the substances mentioned here. “neg,” “pos,” “min,” “max,” and “cor” are the abbreviations for “negative,” “positive,” “minimum,” “maximum,” and “corner,” respectively. “negative” in the first row means “negative slope.” The word in parenthesis means the situation supported by the theory. The unmeasured item is designated as NA.

	H ₂ O	Te	H	Ce	Si	P	S	SnI ₄
anomaly	neg	max	max	min	none	cor	none	cor
slope	neg	NA	neg	pos	(neg)	neg	pos	(neg)

possible errors. The vital point is that no anomaly in the melting curve is recognizable in the LLT region.

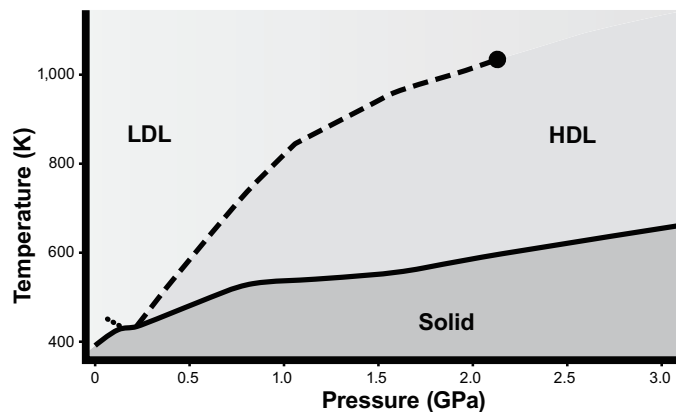


Fig.1 The polyamorphic phase diagram of sulfur. The phase boundary between the LDL and HDL phases (dashed line) determined by *in situ* measurements terminates at the LLCP (black dot), which lies in a pressure–temperature region accessible with ordinary experimental means. The dotted segment near atmospheric pressure indicates the λ -transition line.

Table 1 summarizes the melting curve’s features of the substances mentioned thus far. See also Fig. 2. As mentioned at the beginning of this section, such a thermodynamic anomaly as a melting maximum has guided hunting the substances undergoing an LLT. Most substances indeed have some anomaly, whereas the relevant crystalline phases of silicon and sulfur have a usual melting curve monotonically increasing with pressure (see Fig. 1 for sulfur). Therefore, a melting anomaly is no longer necessary for an LLT to occur. Until the sulfur’s LLT was clarified, Fuchizaki (2013) claimed that not a sign but a discontinuity of the melting curve should be deeply related to an occurrence of LLT. Indeed, based on their *ab initio* simulations, Lee & Lee (2016) found a possibility of LLT in transition metals whose melting curve has a discontinuity in the slope. The sulfur’s LLT requires us to reconsider the proper condition for an LLT.

The other point worth noting is a sign of the slope of the phase boundary between the liquids. The specific volume of HDL should be less than that of LDL

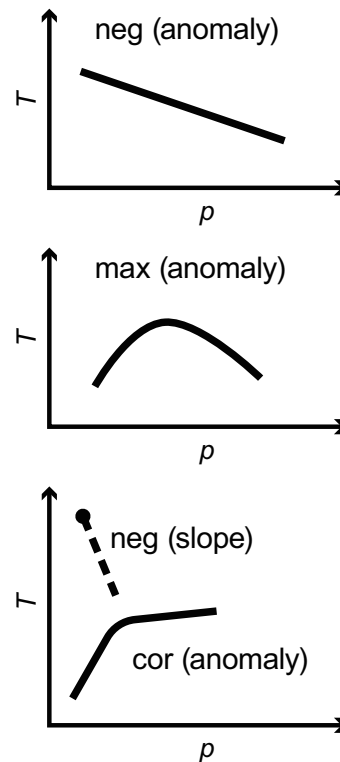


Fig.2 Schematic illustrations for three types of melting curves. A thick line delineated on the pressure (p) – temperature (T) diagram shows a melting curve with the thermodynamic anomaly “neg” (top panel), “max” (middle panel), and “cor” (bottom panel). A melting curve with “min,” convex downward, is not shown. A dashed line terminating at the LLCP (dot) depicts the phase boundary between liquids with a “neg” slope in the bottom panel. For each abbreviation, see Table 1.

(for the former to be of high density). Therefore, the sign depends on the difference in entropy between HDL and LDL. Probably, the specific entropy of an atomic liquid may be higher than that of a molecular liquid with the same specific amount. It is then natural for the phase boundary between molecular H₂ and atomic H liquids to have a negative Clapeyron slope. Molecules in the LDL phase of phosphorus, tin tetraiodide, and sulfur are polymerized in their respective HDL phases. However, the Clapeyron slope of the former two is (supposed to be) negative, whereas sulfur’s slope is evidently positive, as

displayed in Fig. 1. This aspect warns us of an accurate estimate for the entropy of the LDL and HDL phases.

3 Theoretical Approach

We begin with reviewing the prototype theoretical treatment for an LLT. After commenting out the slope of a liquid–liquid phase boundary derivable from the treatment, we go through the recent generalization giving the conclusive scientific basis for water polyamorphism. Other types of theory offering similar conclusions are briefly mentioned. Finally, the author takes up a field-theoretical approach at the beginning of this century, awaiting improvement or modification.

Here, it may be helpful to explain the term “pseudo-binary,” often used in Section 2, as it is the fundamental idea behind the theories. Consider a binary system consisting of two components, A and B. Generally, whether A and B are uniformly mixed depends on thermodynamic conditions and the fraction x of B relative to A. If x is too small, like carbon or silicon in steel, B will be uniformly distributed in A irrespective of thermodynamic conditions; it is rather difficult to extract B in the A matrix. When x increases, B will still be uniformly mixed in A when temperature T is high enough due to the entropy gain. However, it may be difficult for A to accommodate B when T decreases depending on the coupling strength between A–A, B–B, and A–B, giving the solubility limit. Thus, mixing is an interplay between the entropy and energy (more generally, enthalpy when pressure p is an external thermodynamic variable) of mixing.

To this point, B may be a different chemical species from A. In the case of B, which is the same chemical species but with different physical properties such as a specific volume, we call the mixture a pseudo-binary system. The two species specified in Section 2 are nothing but these A and B, forming a pseudo-binary system.

Here and after, we always consider a pseudo-binary mixture of A and B.

3.1 Pseudo-binary regular solution model—the prototype theory

Here, we follow Rapoport’s work (Rapoport (1967)). Rapoport may probably be the first to point out unambiguously a possibility of LLT due to a melting maximum. However, he referred to the essential thermodynamic ingredients in a classical textbook, which is no longer accessible to us. Therefore, we do not faithfully reproduce the derivation but rather

take a shortcut to the conclusions by adopting a more straightforward treatment.

An old theory often treated a fluid as a lattice system; atoms or molecules are located on lattice points. The treatment is still justifiable because the kinetic degrees of freedom do not matter regarding the phase equilibria under consideration. It is essential to focus on the energy and entropy related to configuration.

Each lattice point has z nearest neighbors. We only consider the interactions between the nearest neighbors for simplicity. Among the total lattice points, N , x_i ($i=A, B$) fraction is occupied by the i th species. (No vacant sites are assumed; $x_A + x_B = 1$.) Further, let y_{ij} be the fraction of i – j bonds. ($y_{ij} = y_{ji}$.) Then, the total configurational energy is given by

$$E = \frac{Nz}{2} \sum_{ij} \epsilon_{ij} y_{ij}. \quad (1)$$

Putting $\epsilon_{AA} = -\frac{2}{z}\chi_A$, $\epsilon_{BB} = -\frac{2}{z}\chi_B$, and $\epsilon_{AB} = \epsilon_{BA} = \frac{1}{z}(-\chi_A - \chi_B + \omega)$ after Rapoport, the energy per site is simplified as

$$\epsilon \equiv \frac{E}{N} = -\chi_A x_A - \chi_B x_B + \omega y_{AB}. \quad (2)$$

$\chi(> 0)$ represents the magnitude of attractive interaction of the same kind, whereas ω carries the energy difference between the different species.

For carrying an argument, it is necessary to determine y_{AB} compatible with the given x_A (or x_B). An expedient method invokes the mean-field approximation (the Bragg-Williams approximation (Bragg & Williams (1934)) in materials science). This approximation assumes no correlation between A and B sites so that $y_{AB} = x_A x_B$. The total number of possible arrangements is then $W_{BG} = N! / [(Nx_A)!(Nx_B)!]$, from which we find the configurational entropy per site

$$s = k_B \ln W_{BG} = -k_B [L(x_A) + L(x_B) + 1], \quad (3)$$

where k_B denotes the Boltzmann constant and $L(x) = x \ln x - x$ (whose derivative is $L'(x) = \ln x$).

We have often used the term “regular solution” in Section 2 and the title of this section. A mixed solution whose entropy of mixing takes the form of Eq. (3), which is the entropy of mixing for an ideal solution, is called a regular solution.

Thus, under given conditions of total volume v per site and temperature T , we have the Helmholtz free energy per site:

$$f(v, T) = -\chi_A x_A - \chi_B x_B + \omega x_A x_B + k_B T [L(x_A) + L(x_B) + 1]. \quad (4)$$

Because standard experimental measurements are conducted under constant pressure, we should convert f to the Gibbs free energy through an appropriate Legendre's transform. Formally, we may replace the site energy χ_i with the chemical potential μ_i^0 satisfying $\partial\mu_i^0/\partial p = v_i$, where v_i is the specific volume of species i . The conversion generally needs ω to be a function of p . Thus, we have the Gibbs free energy per site:

$$g(p, T) = \mu_A^0 x_A + \mu_B^0 x_B + \omega(p) x_A x_B + k_B T [L(x_A) + L(x_B) + 1]. \quad (5)$$

Rapoport determined the equilibrium concentration x_A (or x_B) by referring to the old text giving the chemical potential of each species (see Appendix B). Here we take a different route; Regarding g given by Eq. (5) as a function of $x = x_B$, the equilibrium condition $\partial g/\partial x = 0$ yields

$$\frac{\Delta\mu^0}{k_B T} = \ln \frac{x}{1-x} + \frac{\omega}{k_B T} (1-2x), \quad (6)$$

where $\Delta\mu^0 = \mu_A^0 - \mu_B^0$. The mixture with $\omega = 0$ is called an ideal solution. Equation (6) for an ideal solution represents the mass action law for chemical equilibrium upon the reaction $A \rightleftharpoons B$.

The equilibrium concentration x is obtainable by solving Eq. (6) with respect x . The right-hand side (RHS) of Eq. (6) defines the critical temperature

$$T_c = \frac{\omega}{2k_B}. \quad (7)$$

On the low-temperature side, $T < T_c$, Eq. (6) has three solutions, among which two are stable, corresponding to the coexistence of two liquids with either A or B enriched. Rapoport assumed no phase separation and restricted his attention on the high-temperature side $T > T_c$, where Eq. (6) has a single solution x for a given set of p and T .

With this equilibrium fraction x , we find the system's specific volume v through

$$v = \left(\frac{\partial g}{\partial p} \right)_T = v_A - x\Delta v + x(1-x)\gamma, \quad (8)$$

where $\gamma = (\partial\omega/\partial p)_T$ and $\Delta v = v_A - v_B$. We assume that $\Delta v > 0$, i.e., species B is denser. We also evaluate the system's specific entropy s as follows.

$$\begin{aligned} s &= - \left(\frac{\partial g}{\partial T} \right)_p \\ &= s_A - x\Delta s - k_B [(1-x)\ln(1-x) + x\ln x], \end{aligned} \quad (9)$$

where $\Delta s = s_A - s_B$.

The Clausius–Clapeyron relation

$$\frac{dT_m}{dp} = \frac{v - v_s}{s - s_s}$$

then allows us to determine the slope of the melting curve of the solid, which has a melting point T_m and the specific volume and entropy v_s and s_s , respectively, when we substitute Eqs. (8) and (9) for v and s , respectively. The existing dense species may thus make the melting curve decrease, passing through a maximum with increasing pressure.

Rapoport tried to improve the conclusion by adopting the quasichemical approximation, introducing the energetic correlation between species A and B, wholly ignored in the Bragg–Williams approximation, into the number of possible arrangements. The author attains the same result from a level above in Appendix C.

3.2 Phase diagram

Although Rapoport pointed out a possible melting anomaly when a solid melts into a liquid consisting of two species, he did not discuss a possible LLT because there were no direct reports on an LLT at that time. Clear evidence for an LLT of liquid phosphorus has made discussion about phase equilibria between liquids composed of the same chemical components but with different physical properties. Ponyatovsky's work (Ponyatovsky (2003)) probably offered one of the trials to explore a phase diagram involving an LLT based on the pseudo-binary model.

We first note that the left-hand side (LHS) of Eq. (6) can be written as

$$\Delta\mu^0 = \Delta\epsilon^0 - T\Delta s^0 + p\Delta v^0, \quad (10)$$

where Δ refers to the difference between liquid A and B. (Δv defined in Eq. (8) is written with a superscript "0" to stress, like ϵ^0 and s^0 , the quantity of pure liquid A or B.)

Note that the phase equilibrium temperature between liquid A and B, the coexistence temperature of the two liquids, is readily found from Eq. (6) by putting $\Delta\mu^0 = 0$ as

$$T_{\text{cxc}} = \frac{\omega}{k_B} \frac{1-2x}{\ln \frac{1-x}{x}}. \quad (11)$$

We then find the liquid–liquid coexistence pressure, p_{cxc} , by substituting Eq. (11) into Eq. (10).

For a regular solution, T_{cxc} given by Eq. (11) ends up when $x = 1/2$. The terminal temperature, $\lim_{x \rightarrow 1/2} T_{\text{cxc}}$, equals the critical temperature defined

by Eq. (7). The critical pressure p_c is given by substituting Eq. (7) into Eq. (10). The critical point, (p_c, T_c) , thus identified is the LLC. For $T > T_c$, the two liquids, separated in the region below T_c , mix up uniformly, and the coexistence line, along which $x = 1/2$, continues to “devolve” into the so-called Widom line (Holten & Anisimov (2012)).

Ponyatovsky proposed to treat $\Delta\epsilon^0$, Δs^0 , Δv^0 , and even ω as four disposable constants, independent of p and T , to respond to (expected) diverse polyamorphic situations. We then specify the “constant” ω if we can experimentally identify the existing limits of the two liquids because Eq. (5) gives the spinodal lines as

$$\frac{\partial^2 g(p, T)}{\partial x^2} = 0 = -2\omega + \frac{k_B T}{x(1-x)}. \quad (12)$$

Other useful relations directly obtainable from Eq. (6) are the equilibrium temperature and pressure:

$$T(p, x) = \frac{2\omega x - (\Delta\epsilon^0 + \omega + p\Delta v^0)}{k_B \ln \frac{x}{1-x} - \Delta s^0} \quad (13)$$

and

$$p(T, x) = (\Delta v^0)^{-1} \left[2\omega x - (\Delta\epsilon^0 + \omega) - T \left(k_B \ln \frac{x}{1-x} - \Delta s^0 \right) \right]. \quad (14)$$

We have from Eqs. (13) and (14)

$$\left(\frac{\partial x}{\partial T} \right)_p = \frac{k_B \ln \frac{x}{1-x} - \Delta s^0}{2\omega - \frac{k_B T}{x(1-x)}} \quad (15)$$

and

$$\left(\frac{\partial x}{\partial p} \right)_T = \frac{\Delta v^0}{2\omega - \frac{k_B T}{x(1-x)}}, \quad (16)$$

respectively. Equations (15) and (16) are indispensable for estimating the change on the LLT of (the anomalous parts of) the thermal expansion coefficient α , the isothermal compressibility κ_T , and the specific heat at constant pressure c_p as they are given by

$$\Delta\alpha = \frac{\Delta v^0}{v} \left(\frac{\partial x}{\partial T} \right)_p, \quad (17)$$

$$\Delta\kappa_T = \frac{\Delta v^0}{v} \left(\frac{\partial x}{\partial p} \right)_T, \quad (18)$$

and

$$\Delta c_p = (\Delta\epsilon^0 + p\Delta v^0 + \omega - 2x\omega) \left(\frac{\partial x}{\partial T} \right)_p, \quad (19)$$

respectively (Ponyatovsky (2003)).

We see from Eqs. (15) and (16) that $(\partial x/\partial T)_p \rightarrow \infty$ and $(\partial x/\partial p)_T \rightarrow \infty$ as the LLC is approached. Moreover, $(\partial x/\partial T)_p \rightarrow 0$ as T tends to infinity, suggesting that there exists an upper limit x_{\max} of mixing fraction given by $x_{\max} = [1 + \exp(-\Delta s^0/k_B)]^{-1}$.

Ponyatovsky’s proposal was adopted to account for SnI₄ polyamorphism hitherto established experimentally (Fuchizaki et al. (2009)).

On constructing the phase diagram, they noticed the significance of the nonzero enthalpy of mixing, whose magnitude is characterized by ω . The inclusion of the ω -term is essential in arguing polyamorphism. If the strength of ω governs the physics of a given substance’s polyamorphism, the quantities scaled by ω should like similar irrespective of the substance in question. According to this idea, temperature and pressure should be scaled by T_c and p_c , respectively, as well because the value for those critical parameters themselves depends on ω . Let us denote the scaled quantity with a tilde attached to its symbol, e.g., $\tilde{T} = T/T_c$, $\tilde{p} = p/p_c$, $\tilde{\Delta\epsilon}^0 = \Delta\epsilon^0/\omega$, and $\tilde{\Delta s}^0 = \Delta s^0/k_B$.

By this scaling, a quantity defined by

$$\chi \equiv \frac{2\tilde{\Delta\epsilon}^0}{\tilde{\Delta s}^0}, \quad (20)$$

which they called the energy–entropy competition parameter, came to the front. For example, the equilibrium criterion, Eq. (6), now takes the scaling form:

$$\frac{\tilde{\Delta s}^0}{2} \left[(\chi - \tilde{T}) - \tilde{p}(\chi - 1) \right] + (1 - 2x) + \frac{1}{2} \tilde{T} \ln \frac{x}{1-x} = 0,$$

implying $x = x(\tilde{p}, \tilde{T}; \chi, \tilde{\Delta s}^0)$. Hence, all Ponyatovsky’s parameters are not independent; to determine the pressure and temperature dependence of x , we merely specify $\tilde{\Delta\epsilon}^0$ and $\tilde{\Delta s}^0$.

It should be emphasized that the scaling picture can bring a “universality” in dictating the polyamorphic phase equilibria. Here, the author used the term “universality” somewhat loosely; it is universal up to a choice of χ and $\tilde{\Delta s}^0$.

First of all, the phase boundary of an LLT given by Eq. (10) can be transformed into

$$\tilde{T}_{\text{cxc}} = (1 - \chi)\tilde{p} + \chi, \quad (21)$$

which is a line with a slope $1 - \chi$ and an intercept χ on the \tilde{p} – \tilde{T} phase diagram. The lower part of the line below $\tilde{T} = 1$ (i.e., $T \leq T_c$) represents the equilibrium phase boundary, whereas the upper part is the metastable extension corresponding to the Widom line.

Recall the slope of the LLT boundary summarized in Table 1. If $\chi > 1$, the slope becomes negative while it becomes positive when $\chi < 1$. We call the former (latter) case energetic (entropic) because the energy (entropy) difference dominates in determining the slope's sign. Thus, not only the entropy difference between the two species but also the energy difference does matter. It is important to realize that the energy is given in units of ω . Because χ , the intercept of the line, Eq. (21), should be positive definite, Δs^0 has the same sign as that of $\Delta \tilde{\epsilon}^0$, whose sign depends on the sign of both $\Delta \epsilon^0$ and ω . The LLT line could take a positive or negative slope upon the polymerization of a molecular liquid (see Table 1). This fact implies that we should simultaneously consider the difficulty (easiness) of mixing and the change in morphology of the two species.

Secondary, the spinodal lines determined from Eq. (12) are explicitly given as follows (Fuchizaki et al. (2011)):

$$\tilde{p}_{\pm} = \frac{\chi}{\chi - 1} \pm \frac{2\sqrt{1 - \tilde{T}}}{(\chi - 1)\Delta \tilde{s}^0} - \frac{1}{\chi - 1} \left(1 + \frac{1}{\Delta \tilde{s}^0} \ln \frac{1 \pm \sqrt{1 - \tilde{T}}}{1 \mp \sqrt{1 - \tilde{T}}} \right) \tilde{T}. \quad (22)$$

Fuchizaki et al. (2009) showed the “universal” phase diagram thus constructed. Assuming the value for χ (i.e., the magnitude of the slope) and either of T_c or p_c fixes the actual units of the phase diagram. Furthermore, if the existing limits of A and B at low temperatures are available, Δs^0 is completely determinable as the spinodal lines, given by Eq. (22), intersect the \tilde{p} -axis at $(\chi \pm 2/\Delta \tilde{s}^0)/(\chi - 1)$. (For details, see Fuchizaki et al. (2009), in which $p_c = 0.5$ GPa for SnI_4 was assumed. This assumption was found inappropriate and corrected to $p_c = 1.3$ GPa in Fuchizaki et al. (2011). Then, $T_c = 970$ K resulted, giving a consistent interpretation for all the experimental measurements.)

3.3 Unification

We have reviewed the thermodynamics of polyamorphism based on Rapoport's theory Rapoport (1967) up to here. Recall that Rapoport restricted himself to the case of no phase separation between the constituent “species.” Although isotropic liquid crystal transforms to nematic liquid crystal phase via a discontinuous transition without phase separation, the HDL phase is separated from the LDL in liquid phosphorus and sulfur (see Sections 2.6 and 2.7). Therefore, we do not

necessarily impose a limitation on an allowable temperature range.

Another important thing is that we have entirely neglected the background thermodynamics of a general fluid, which undergoes a liquid–gas transition (LGT). Indeed, it became apparent that the type of polyamorphic scenario emerging is determined by the interplay between an LLT and LGT, as seen below.

To the author's knowledge, Anisimov et al. (2018) may be the first to give unified thermodynamics, considering the background thermodynamic effects into the pseudo-binary regular solution model. (Stokely et al. (2010) have noticed the essential significance of including the background effects, but their treatment was limited to the water case, which is briefly touched on Section 3.4.) They could suitably incorporate the background thermodynamics, reinterpreting the “chemical reaction” between “species” A and B in terms of the phase-transition language describing a symmetry breaking.

Let us adapt the pseudo-binary regular solution model to the Ginzburg–Landau-type theory of phase transitions (Hohenberg & Krekhov (2015)), describing the change in order phenomenologically. The order reflecting the system's symmetry, described by a quantity called the order parameter, plays a central role in the theory. Let us denote the order parameter and the conjugate field breaking a higher symmetry by ϕ and h , respectively. (ϕ is not necessarily a scalar and could be a vector if the ordered state is describable by two components. Then, the corresponding field is also a vector. In the isotropic to nematic liquid transition mentioned above, ϕ becomes a tensor specifying the anisotropy. We symbolically write the order parameter and field as ϕ and h in any case for simplicity. Unless otherwise explicitly stated, (the magnitude of) ϕ takes a value between zero (completely disordered) and unity (completely ordered).) In terms of ϕ , the Ginzburg–Landau free energy per molecule generally reads as

$$G(p, T, \phi) = g_0(p, T) + k_B T g_{\text{sym}}(\phi) - h\phi. \quad (23)$$

g_0 is the free-energy density representing the background thermodynamics whereas g_{sym} carries the symmetry to be broken by the field h .

The ingenuity of Anisimov et al. (2018) was casting Eq. (5) into the form given by Eq. (23), identifying that the “field” should be the difference in the free energy (chemical potential), $g_B - g_A$, between the two “species” (see Fig. 3). Then, we can rewrite Eq. (5) as

$$g(p, T, x) = g_A(p, T) + g_{\text{mix}} + g_{\text{BA}}x. \quad (24)$$

Viewing Eq. (23) as Eq. (24) corresponds to a translation of the language from phase transition to chemical reaction $A \rightleftharpoons B$. The fraction x , taken as the order parameter, is called the reaction coordinate, representing the degree of reaction in the chemical reaction language. Note that we took species A as the reference state. g_A should carry the background thermodynamics and takes care of the LGT occurring in pure liquid A. g_{mix} represents the mixing part of the free energy, whose form is found from a comparison with Eq. (5) as

$$g_{\text{mix}} = \omega x(1-x) + k_B T [x \ln x + (1-x) \ln(1-x)],$$

where the first and second terms are the mixing enthalpy and entropy contribution of a regular solution.

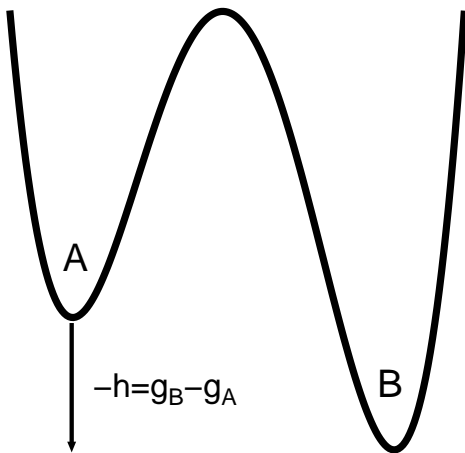


Fig.3 Schematic view of the free energy after a symmetry is broken by field h . Anisimov et al. (2018) regarded the free energy for state B relative to A as the symmetry-breaking field.

The chemical-reaction equilibrium condition $(\partial g / \partial x)_{p,T} = 0$ then again yields

$$\begin{aligned} h &= k_B T \ln K(p, T) = -g_{BA}(p, T) \\ &= k_B T \ln \frac{x}{1-x} + \omega(1-2x), \end{aligned} \quad (25)$$

which is Eq. (6) in the chemical reaction language. (Previously, we referred the state relative to state B, and thus $-g_{BA} = \Delta\mu$. Here we suppress the superscript “0” representing a pure state to avoid an unnecessary complexity.) K is known as the reaction equilibrium “constant” (see also Eq. (C.5)) (although a function of p and T in general). The solution to Eq. (25), when substituted in Eq. (24), then gives the equilibrium free energy that can capture all the phase behavior including a vapor phase.

We have to determine or assume the functional form for g_{BA} to go beyond this point. Generally, g_{BA} will

take the form

$$\begin{aligned} g_{BA}(p, T)(= \Delta\mu) &= \Delta\epsilon + p\Delta v - T\Delta s \\ &+ pT\Delta\alpha + p^2\Delta\kappa_T + T^2\Delta c_p + \dots, \end{aligned} \quad (26)$$

where $\Delta\epsilon$, Δv , Δs , $\Delta\alpha$, $\Delta\kappa_T$, and Δc_p are the changes (in a first approximation) of energy, volume, entropy, isobaric expansivity, isothermal compressibility, and heat capacity (in suitable dimensions), respectively, in the reaction $A \rightarrow B$. Anisimov et al. (2018) adopted the linear terms in Eq. (26) in their discussion and treated $\Delta\epsilon$, Δv , and Δs as constants. They also assumed that ω is a constant independent of p and T . It needs to specify the reference $g_A(p, T)$, to which they employed two choices: the chemical potential of the lattice-gas model and that of the van der Waals fluid. Irrespective of the qualitative difference between these choices (the lattice-gas model has two “species,” empty and occupied sites, whereas the van der Waals fluid has no such interconvertible species), the same result was qualitatively obtainable for the phase diagram.

In Anisimov et al.’s treatment, the LLCPC location is at our disposal. They thus obtained the quite general consequence regarding the phase behavior upon an LLT (under the employment of the lattice-gas model or the van der Waals fluid as a reference state). They revealed that what scenario comes out among the possible ones, a singularity-free scenario (Sastry et al. (1996)), a common LLPT scenario (Poole et al. (1992)), or an LLPT-free scenario (Angell (2008)) proposed for water polyamorphism, depends on the location of the LLCPC and the magnitude of $\Delta\epsilon$. Stokely et al. (2010) has already reached the same conclusion but with the specific water model. Anisimov et al.’s unified view also clarified that the LLCPC-free scenario is a variant of the stability limit conjecture, which has been proposed for water previously (Speedy (1982)). The LLPT scenario realizes when an LLCPC appears in a positive temperature region below the absolute stability limit of a liquid state to vapor. Thus, the very existence of the LLCPC (though not accessible to us) is shown to result in water polyamorphism.

Their treatment also allowed us to calculate the pattern of the extrema loci of density, isothermal compressibility, and isobaric heat capacity. Because these quantities are given as a function of $p(x)$ and $T(x)$, we can obtain the loci by eliminating x , a solution to Eq. (25). The appearance of the loci on the p - T phase diagram depends on the location of both the LLCPC and liquid-gas critical point. Therefore, even though the LLCPC lies in the no man’s land, the validity of

the LLCPC scenario could be supported (indirectly) if we experimentally confirm the shape and location of those extrema loci. (This proposal has already been suggested by Franzese & Stanley (2007) from their calculations using the water model, which was subsequently adopted by Stokely et al. (2010).)

3.4 Other indispensable contributions

In this subsection, the author introduces quite a different approach worth mentioning. The approach is exceedingly legitimate in statistical mechanics; one first constructs a microscopic model and then evaluates the partition sum of the desired thermodynamic quantities. The starting microscopic model is thus legitimately coarsened to obtain a thermodynamic description, which is equivalent to the pseudo-binary regular solution model discussed thus far. This subsection is closed by itself in this context. We get back on track in the following subsection.

Two such trials are mentioned; the first is due to Russian physicists led by A. Z. Patashinski, and the other is from the Western side, whose leader was H. E. Stanley.

Patashinski and his coworkers have discussed melting from a microscopic point of view (Mituš & Patashinski (1982), Patashinski & Ratner (1997)). Son et al. (1998) considered that an order–disorder transition is a melting of an ordered state and embedded a model undergoing the order–disorder transition in a system with a phase transition between different phases.

The starting situation is somewhat similar to that of Rapoport’s in that we consider a lattice model but is definitely different in that Son et al. (1998) treated the configuration microscopically. They explicitly assigned the site \mathbf{r} at which a cluster with definite molecular orientation inherent in the crystalline state is located. (Even if the orientational correlations are lost at high temperatures, a cluster keeps its shape. This aspect is justifiable for a molecule with strong covalent or hydrogen bonding such as phosphorus, sulfur, or water.) A cluster’s state at \mathbf{r} is then described by a pseudo-spin $\sigma^k(\mathbf{r})$, where the orientation specified by k can take N varieties with the same energy. The specification of orientation is such that $\sigma^k = 1$ when a cluster takes the k th orientation and otherwise, $\sigma^k = 0$. In statistical physics, such a model consisting of N degenerated pseudo-spins is called an N -state Potts model (Wu (1982)). As in Rapoport’s treatment, we further assume each $\sigma_i(\mathbf{r})$ can take two states (“species”) A and B with different energies. Again, let the fraction of species B be

x . After very lengthy statistical-mechanical calculations of coarse-graining, Son et al. (1998) obtained the following free energy per site:

$$\begin{aligned}
 g(p, T, x) = & -J_1(1-x)^2 \left(\varphi_1 - \frac{\varphi_1^2}{2} - \frac{(1-\varphi_1)^2}{2(n-1)} \right) \\
 & - J_2x^2 \left(\varphi_2 - \frac{\varphi_2^2}{2} - \frac{(1-\varphi_2)^2}{2(m-1)} \right) \\
 & - \omega x(1-x) - hx \\
 & + k_B T [(1-x) \ln(\varphi_1(1-x)) + x \ln(\varphi_2x)].
 \end{aligned} \tag{27}$$

Here, φ_i is the spatial average for the pseudo-spin in state A ($i = 1$) or B ($i = 2$) with the spin degeneracy n ($i = 1$) or m ($i = 2$). Note that φ_i equals the probability of finding a cluster in the state specified by i . (We treat φ_i as not the spatial average but the local order in Section 3.5.) The pressure dependence enters through the energy parameters between the same states J_i , between the different states ω , and the external field h . Those pressure dependences were treated only phenomenologically by introducing several adjustable parameters to be compatible with the experimental results. Here, we call the coarse-grained model with the free energy given by Eq.(27) the mixed Potts model.

Fuchizaki et al. (2011) applied Eq. (27) to explain the SnI_4 polyamorphism with great success. By choosing the p -dependent adjustable parameters appropriately, they could semiquantitatively reproduce the location of polyamorphic phase transitions determined by the pseudo-binary regular solution model. They also predicted the phase boundary between the polymorphs. Surprisingly, the mixed Potts model gave the quantitatively same LLCPC location as the pseudo-binary regular solution model.

Stanley and his coworkers have discussed the thermodynamic anomalies in water for years based on a kind of lattice–gas model specific to a water system (Franzese & Stanley (2002), Franzese et al. (2003), Franzese & Stanley (2007)). As in the usual lattice gas model, let us introduce the occupation variable $n_{\mathbf{r}}$, which takes $n_{\mathbf{r}} = 1$ (0) when the site at \mathbf{r} is occupied (empty) by a water molecule. They gave the following Hamiltonian.

$$\begin{aligned}
 H = & -J_0 \sum_{\langle \mathbf{r}, \mathbf{r}' \rangle} n_{\mathbf{r}} n_{\mathbf{r}'} - J \sum_{\langle \mathbf{r}, \mathbf{r}' \rangle} n_{\mathbf{r}} n_{\mathbf{r}'} \delta_{\sigma_{\mathbf{r}\mathbf{r}'}, \sigma_{\mathbf{r}'\mathbf{r}}} \\
 & - J_{\sigma} \sum_{\mathbf{r}} n_{\mathbf{r}} \sum_{(k,l)_{\mathbf{r}}} \delta_{\sigma_{\mathbf{r}k}, \sigma_{\mathbf{r}l}}
 \end{aligned} \tag{28}$$

The first term, where $J_0 (> 0)$ carries the strength of the van der Waals attraction, and the sum is taken

over the nearest neighbor pairs at \mathbf{r} and \mathbf{r}' , is the ordinary lattice-gas model Hamiltonian taking on the LGT. In the second term of Eq. (28), $\sigma_{\mathbf{r}\mathbf{r}'}$ represents a q -state Potts pseudo-spin corresponding to a number of q possible orientations of a water molecule. The pseudo-spins were introduced to describe the interaction energy due to hydrogen bonding. Two molecules in the nearest neighbor cells at \mathbf{r} and \mathbf{r}' can form a hydrogen bond only if they are correctly oriented. The Kronecker delta symbol is used to express this condition. Thus, $J(> 0)$ represents the strength of a hydrogen bond. The third term in Eq. (28), the intramolecular term, ensures that water molecules are kept unbroken. A water molecule has four arms for hydrogen bonding. For each of the six different pairs $(k, l)_{\mathbf{r}}$ of the arms of a molecule at site \mathbf{r} , the Kronecker delta ensures the intramolecular bonding with the strength $J_{\sigma}(> 0)$.

They solved Eq. (28) using the mean-field approximation and Monte Carlo simulation and confirmed the LLCP scenario for water polyamorphism. They also showed the locus of temperature maximum consistent with the experimental results.

Stokely et al. (2010) performed an extensive calculation using Eq. (28) for a wide range of parameters J and J_{σ} and found (prior to Anisimov et al. (2018)) that singularity-free, LLPT, and LLPT-free scenarios for water are all correct. The appropriate choice of J and J_{σ} (in units of J_0) finally determines the actual scenario. A superficial comparison of Stokely et al.'s result with Anisimov et al.'s offers J and J_{σ} correspond to $\Delta\epsilon$ and ω . However, this correspondence should be further scrutinized.

3.5 Field-theoretic approach

We have thus far described the thermodynamics of polyamorphism mainly based on the pseudo-binary regular solution model. We took the free-energy density (the free energy per site) given by Eq. (5) as the basis of our discussion. We saw that the mixed Potts models are also reducible to a similar form of the free-energy density. Those densities were functions of x ($= x_B$) as well as of the thermodynamic variables, p and T . In a real system, species B is never distributed uniformly. That is, x depends on a location \mathbf{r} within a system. Therefore, precisely stating, the free-energy density should be a functional of $x(\mathbf{r})$. Tanaka (2000) has already extended the argument during the early years of theoretical development. Here, the author introduces his basic idea.

The fraction x , playing the central role of the discussion thus far, is called an order parameter in the

phase-transition language. A choice of the order parameters is at our disposal as far as they are relevant to describing the phase transition under consideration. In general, it is natural to assume, as was assumed in the mixed Potts model, multiple states for the locally favored structure in a liquid. Tanaka (2000) adopted the bond-orientational order (Steinhardt et al. (1983)) to capture the locally favored structure, which we denote by $\varphi(\mathbf{r})$. Unlike the fraction x , φ is not necessarily conserved. We presume that q_{φ} states are associated with the local state $\varphi(\mathbf{r})$.

We have to include the density ρ as a conserved order parameter, which is necessary to describe the state of a fluid. The degeneracy q_{ρ} associated with the state specified by ρ should be much larger than q_{φ} . It is easier to imagine that ρ governs the global order (although it is defined as a local quantity). The entropy density for the whole system is then given by

$$s(\varphi) = -k_B \left[\varphi \ln \frac{\varphi}{q_{\varphi}} + (1 - \varphi) \ln \frac{1 - \varphi}{q_{\rho}} \right],$$

which is a generalization for the crudest description given by Eq. (3).

The local energies ϵ_{ρ} and ϵ_{φ} should satisfy the relation $\Delta\epsilon \equiv \epsilon_{\rho} - \epsilon_{\varphi} > 0$ as we assume that the state corresponding to φ is locally favorable. Then, Eq. (2) is generalized to

$$\epsilon(\varphi) = \varphi\epsilon_{\varphi} + (1 - \varphi)\epsilon_{\rho} + \omega\varphi(1 - \varphi).$$

Tanaka considered that a local order introduces some ‘‘frustration’’ to the global order and assumed $\omega > 0$.

Finally, we have to consider the work done on the system by external pressure, the one corresponding to the final term of Eq. (10). Notice that the mixed state’s characteristic volume is given by $\varphi v_{\varphi} + (1 - \varphi)v_{\rho}$; the work in question is obtainable by multiplying p to this volume. Tanaka set $\Delta v \equiv v_{\varphi} - v_{\rho} > 0$ assuming the case of water.

Combining these contributions, we can write the system’s free energy as the following Ginzburg–Landau functional form:

$$\mathcal{H}[\varphi] = \int d\mathbf{r} g(p, T, \varphi(\mathbf{r})), \quad (29)$$

where the free-energy density now takes

$$\begin{aligned} g(p, T, \varphi) = & \varphi\epsilon_{\varphi} + (1 - \varphi)\epsilon_{\rho} + \omega\varphi(1 - \varphi) \\ & + k_B T \left[\varphi \ln \frac{\varphi}{q_{\varphi}} + (1 - \varphi) \ln \frac{1 - \varphi}{q_{\rho}} \right] \\ & + [\varphi v_{\varphi} + (1 - \varphi)v_{\rho}] p. \quad (30) \end{aligned}$$

The equilibrium value of φ is found from the condition $\delta\mathcal{H}/\delta\varphi = 0$, leading

$$\frac{1}{k_{\text{B}}T} [-\Delta\epsilon + p\Delta v + \omega(1 - 2\varphi)] + \ln \frac{q_{\rho}\varphi}{g_{\varphi}(1 - \varphi)}, \quad (31)$$

which should be compared with Eq. (6). It is easy to verify that $\varphi = 1/2$ gives the LLC. Equation (7) again gives the critical-point temperature, below which the system undergoes the LLT, whose temperature is

$$T_{\text{cxc}} = \frac{1}{\Delta v} (\Delta\epsilon - T_{\text{c}}\Delta s) \quad (32)$$

where $\Delta s = k_{\text{B}} \ln(q_{\rho}/q_{\varphi}) (> 0)$ representing a loss of entropy when a part of the liquid with order ρ is substituted by a liquid with order φ . Equation (21) is thus updated.

An interesting point worth noting is that various outcomes are obtainable for the appearance of polyamorphism depending on the magnitude of $\Delta\epsilon$ and ω . When both $\Delta\epsilon$ and ω are large, the LLC will be located in a liquid state, and a thermodynamically stable LLT is observable. If their values are small, the LLC will be located on the negative pressure side in case of $\Delta v > 0$. The LLT, if it occurs at a low temperature, might then be hidden by a liquid-glass transition. When a system has intermediate values of $\Delta\epsilon$ and ω , the LLC and the associated LLT will exist in a metastable state below the melting curve. Tanaka (2000) conjectured that water belongs to this class.

4 Concluding remarks

We have seen a process of theoretical development for the thermodynamical survey of polyamorphism. The process seems quite right as one of the examples for constructing a theory of phase transitions, which is usually initiated with a model with a uniform order parameter. A first trial to obtain a closed equation for the order parameter is invoking the mean-field approximation to factorize the nonlinear correlations between the order parameters. Rapoport (1967) opened this first entrance. However, it took more than 30 years to broaden his scope further until the discovery of a substance undergoing a thermodynamically stable LLT. Other substances in Section 2 basically support the initial point of view, leading to a critical-point scenario. The recently updated version of the theory could unify the various scenarios for explaining the water polyamorphism into the critical-point scenario, as seen in Section 3; the critical-point scenario can take the other shapes, i.e., the other scenarios, depending on the location of an LLC in the p - T phase

diagram. The thermodynamics of polyamorphism is thus reduced to that of a critical point near which the correlation between local fluctuations governs the system's essential response. Therefore, it is natural to employ a field-theoretic description. This situation requires us to (re)consider a Ginzburg-Landau type formalism.

The formulation put forth by Tanaka (2000) may provide us with a good starting point. Here, the author proposes the issues to be deliberated.

The first one should be the mixing enthalpy. Tanaka (2000) has restricted, assuming a structural discordance between the matrix and a lower-density structure, to the case of positive ω . As pointed out in Section 3.2, the sign of ω could determine the slope's sign of an LLT line. Therefore, we need to quantitatively evaluate the structural coherence between the matrix liquid and a droplet of the lower-density (molecular) liquid, conducting, for example, first-principles calculations. In the author's view, the morphology difference between the two "species" would matter in assessing the difference between not only the entropy but also the enthalpy affecting the sign and magnitude of the slope in question (see Section 3.2). Addressing this issue would resolve the problem of taking a different sign upon the LLT from molecular to polymerized liquid, posed in Section 2.9.

The second issue is somewhat related to the first but undoubtedly concerns phase-transition kinetics. The pseudo-binary regular solution model only deals with the relative fraction of the two "species." The mixed Potts model, generalized to treat multiple rather than two states, could include the effects of a liquid-gas transition an ordinary fluid undergoes. The generalization attained by Anisimov et al. (2018) could enhance the original pseudo-binary regular solution model to incorporate those effects. Tanaka (2000) extended the pseudo-binary regular solution model, as seen in Section 3.5. Instead of the relative fraction, he chose q_{φ} degenerated orientations to specify the local order $\varphi(\mathbf{r})$ of a fluid at \mathbf{r} and derived the equation satisfied by the spatially averaged φ . We then have to consider fluctuations $\delta\rho(\mathbf{r})$ and $\delta\varphi(\mathbf{r})$ from the average density ρ and φ , respectively. $\delta\rho$ can be assumed to fluctuate around the average. It is appropriate for $\delta\varphi$ to assume a nonzero value below some temperature, at which the higher spatial symmetry $\delta\varphi = 0$ is broken (Hohenberg & Halperin (1977)). The problem is that we cannot *a priori* know the coupling scheme $h(\delta\rho, \delta\varphi)$ between the fluctuations of the conserved and nonconserved order parameters. This coupling scheme has been categorized as

model C by Hohenberg & Halperin (1977). The time-dependent Ginzburg–Landau description for model C then leads to the following time-evolution equations for the fluctuations (Tanaka (2000)):

$$\begin{aligned}\frac{\partial\delta\rho(\mathbf{r},t)}{\partial t} &= L_\rho\nabla^2\left[-K_\rho\nabla^2\delta\rho + \frac{\partial h(\delta\rho,\delta\varphi)}{\partial\delta\rho(\mathbf{r},t)}\right], \\ \frac{\partial\delta\varphi(\mathbf{r},t)}{\partial t} &= -L_\varphi\left[-K_\varphi\nabla^2\delta\varphi + \frac{\partial h(\delta\rho,\delta\varphi)}{\partial\delta\varphi(\mathbf{r},t)}\right].\end{aligned}$$

Here, L s are kinetic coefficients, whereas K s control the interfacial energy of fluctuations.

Thus, one of the ways with which to determine $h(\delta\rho,\delta\varphi)$ is to measure the frequency response of the density and bond-orientation relaxations. Application of femtochemistry (Dantus & Zewail (2004)) may be one of the triggers that leads us to find the answer.

We have seen the forest of polyamorphism from some specific trees. They are all related to fluids. The author considers that even an ultimately exact theory for the thermodynamics of polyamorphism cannot answer the necessary condition for an LLT. Solving whether a melting anomaly (see Table 1) is relevant to an LLT will need to consider the thermodynamics of a solid phase as well; polyamorphism of a substance must be inextricably intertwined with its polymorphism.

Acknowledgments

This work was supported by JSPS KAKENHI (Grant Nos. 17K05581 and 20K03790).

Appendix A Reverse Monte Carlo analysis

Suppose we measure an isotropic substance without long-range order, such as liquid or amorphous material, by diffraction using a probe with a wavelength equal to an order of intermolecular or interatomic distance. In that case, we can obtain the structure factor $S(k)$. Because $S(k)$, the relative diffraction intensities as a function of wavenumber k , is one-dimensional information, we only obtain the one-dimensional structural aspect along the radial distance r when we transform $S(k)$ back to real-space information. We can estimate the coordination numbers of the nearest neighbors or the next nearest neighbors at most.

If we desire to know three-dimensional structural aspects such as actual packing fashion or orientation of molecules, we need to carry out simulations; we (re)arrange the constituent molecules or atoms in a trial-and-error fashion until we obtain the measured $S(k)$. This simulation technique is called the reverse Monte Carlo (RMC) method (McGreevy (2001)). If we could know *a priori* some local information such

as bond lengths or bond angles of molecules, we may employ them as the constraints during the simulation. Structural analysis using RMC as a dominant tool is often called the RMC analysis for short. The method has been well matured and is applied for structural analysis of a wide range of substances (Gereben & Pusztai (2012)).

Two kinds of information are required to conduct RMC analyses beforehand. One is the density of the substance to be analyzed, and the other is an initial molecular arrangement. In particular, assessing the density of non-crystalline substances is not a trivial task if a macroscopic method such as pycnometry is not applicable. Some methods trying to estimate the density from $S(k)$ itself have been proposed (Eggert et al. (2002), Fuchizaki et al. (2007), Sakagami et al. (2016)). Preparing a proper initial arrangement is also essential; if it is far apart from the actual structure, the simulation will not converge or, in even a worse situation, will be trapped by a false structure with a similar $S(k)$.

The RMC analysis result is sometimes controversial, especially when the result gives a new structure because the method does not have a firm physical basis. *Ab initio* calculations, if available, can give helpful support for justifying the RMC result. It is accessible from the RMC result to derive the one-dimensional information, i.e., the radial distribution function, which should be compared with the one directly obtainable from a Fourier inversion of $S(k)$. The confirmation might be meaningful whether the RMC result is reliable.

Appendix B Chemical potential

Rapoport (Rapoport (1967)) cited an old textbook, to which most of us are probably inaccessible, for the chemical potential. Here the author reproduces the expression through simple mathematic manipulation.

First, we rewrite the free energy to expose the symmetry involved in exchanging species A and B by introducing a new variable $\phi = 1/2 - x_B$. Then, Eq. (5) gives

$$\begin{aligned}g(p,T,\phi) &= \left(\frac{1}{2} + \phi\right)\mu_A^0 + \left(\frac{1}{2} - \phi\right)\mu_B^0 \\ &+ k_B\left[\left(\frac{1}{2} + \phi\right)\ln\left(\frac{1}{2} + \phi\right)\right. \\ &+ \left.\left(\frac{1}{2} - \phi\right)\ln\left(\frac{1}{2} - \phi\right)\right] \\ &+ \left(\frac{1}{2} + \phi\right)\left(\frac{1}{2} - \phi\right)\omega, \quad (\text{B.1})\end{aligned}$$

which is an even function of ϕ on exchanging A and

B.

Thermodynamics tells us that the free energy per site should be

$$g(p, T) = x_A \mu_A + x_B \mu_B. \quad (\text{B.2})$$

Regarding Eqs. (B.1) and (B.2) as identities for ϕ , we readily find

$$\mu_A = \mu_A^0 + k_B T \ln \left(\frac{1}{2} + \phi \right) + \left(\frac{1}{2} - \phi \right)^2 \omega \quad (\text{B.3})$$

and

$$\mu_B = \mu_B^0 + k_B T \ln \left(\frac{1}{2} - \phi \right) + \left(\frac{1}{2} + \phi \right)^2 \omega \quad (\text{B.4})$$

because the last term on the RHS of Eq. (B.1) is modified as $(1/2 + \phi)(1/2 - \phi)\omega = [(1/2 + \phi)(1/2 - \phi)(1/2 + \phi + 1/2 - \phi)]\omega$.

Equations (B.3) and (B.4) are Eqs. (G.4.05.2) and (G.4.05.4), respectively, in Rapoport's paper. He required equating μ_A and μ_B for the system to achieve equilibrium to arrive at Eq. (6).

Because of the even parity of $g(p, T, \phi)$ given by Eq. (B.1), the derivative concerning ϕ becomes an odd function, implying that the derivative always passes through the origin. That is, $\phi = 0$ is the fixed point. In terms of the original variable, the RHS of Eq. (6) passes through $x = 1/2$ whatever ω and T are.

Appendix C Quasichemical approximation

A statistical mechanical approach for a phase transition often starts with a mean-field theory to grasp an overview of the transition. A mean-field theory entirely neglects the effects of fluctuations associated with the correlations among the constituents. Therefore, it can predict an overall thermodynamic aspect at high temperatures or in high space dimensions, where fluctuations do not matter. However, it fails to predict even a qualitative feature close to a critical point or in low space dimensions, where fluctuations dominate phase behavior.

Thus, the next step is incorporating the correlations between the components. It is no exaggeration to say that equilibrium statistical mechanics have been devoted to developing practical tools to deal with fluctuations.

For example, a strategy goes as follows. We first correctly incorporate the correlations between the nearest neighbors while the two beyond the nearest neighbors are treated in a mean-field fashion. Such a treatment can be extended successively, incorporating

the exact correlations between the next-nearest neighbors. One of the goals in this direction has been the cluster variation method (CVM) (Kikuchi (1951)).

The CVM *approximately* modifies the coarsest estimate W_{BW} for the number of possible arrangements of species A and B on the lattice as

$$W_{\text{CVM}} = W_{\text{BW}} (G_{\text{pair}})^\alpha, \quad \alpha = \frac{z}{2} \quad (\text{C.1})$$

with the correlation correction factor given by

$$G_{\text{pair}} = \frac{(\prod_i (N x_i)!)^2}{\prod_{ij} (N y_{ij})! N!}. \quad (\text{C.2})$$

The entropy per site given by Eq. (3) is now updated as

$$\begin{aligned} s &= k_B \ln W_{\text{CVM}} \\ &= k_B \left[(2\alpha - 1) \sum_i L(x_i) \right. \\ &\quad \left. - \alpha \sum_{ij} L(y_{ij}) + (\alpha - 1) \right], \quad (\text{C.3}) \end{aligned}$$

which then rewrites the specific free energy as

$$\begin{aligned} g(p, T) &= \mu_A^0 x_A + \mu_B^0 x_B + \omega y_{AB} \\ &\quad - k_B T [(2\alpha - 1) (L(x_A) + L(x_B)) \\ &\quad - \alpha (L(y_{AA}) + L(y_{BB}) + 2L(y_{AB})) + (\alpha - 1)]. \quad (\text{C.4}) \end{aligned}$$

Recall that the fraction of A–B pairs was approximated as $y_{AB} = x_A x_B$ in the mean-field treatment. The more probable fraction can be found as the one that minimizes g given by Eq. (C.4). Thus,

$$\frac{\partial g(p, T)}{\partial y_{AB}} = \omega + \alpha k_B T \ln \frac{y_{AB}^2}{y_{AA} y_{BB}},$$

or

$$\frac{y_{AB}^2}{y_{AA} y_{BB}} = \exp \left(-\frac{\omega}{\alpha k_B T} \right) \equiv \eta^{-2}. \quad (\text{C.5})$$

Because of $y_{AA} = x_A$ and $y_{BB} = x_B - y_{AB}$, Eq. (C.5) constitutes a quadratic equation for y_{AB} , and the physically meaningful solution is easily obtainable as

$$y_{AB} = \frac{[4(\eta^2 - 1)x_A x_B]^{\frac{1}{2}} - 1}{2(\eta^2 - 1)}. \quad (\text{C.6})$$

Equation (C.5) is interpreted to represent the relationship among the (molar) fractions involved in the chemical reaction $A_2 + B_2 \rightleftharpoons 2AB$ with the reaction energy ω/α . Hence, the treatment leading to

Eq. (C.5) has been named quasichemical approximation. However, current advanced textbooks regarding statistical mechanics rarely refer to such treatment, even the powerful CVM, especially as far as a phase transition is concerned. The accomplishment of renormalization-group theory (Wilson (1971*a,b*)), prescribing the *exact* and systematic way of incorporating fluctuations near a critical point, has made those approximations things of the past.

Let us discuss the equilibrium condition under the present approximation differently from that given by Rapoport. We focus on the grand potential Ω , which involves desired chemical potentials. The reduced grand potential per site is given by

$$\begin{aligned} \psi \equiv \frac{\beta\Omega}{N} = & \beta\alpha \sum_{ij} \epsilon_{ij} y_{ij} \\ & - \frac{1}{2}(2\alpha - 1) \left[\sum_i L(x_i) + \sum_j L(x_j) \right] \\ & + \alpha \sum_{ij} L(y_{ij}) - (\alpha - 1) - \frac{1}{2}\beta \left(\sum_i \mu_i x_i + \sum_j \mu_j x_j \right) \\ & + \beta\lambda \left(1 - \sum_{ij} y_{ij} \right), \end{aligned}$$

where $\beta = (k_B T)^{-1}$ and λ is an undetermined multiplier. Note here that the sum over i is divided into i and j to make the expression symmetric on exchanging i and j . $-\chi_A$ ($-\chi_B$) in ϵ_{AA} (ϵ_{BB}) was replaced by μ_A^0 (μ_B^0). For a given x_B (or x_A), $\{y_{ij}\}$ are those that make ψ minimum and are determined from

$$\begin{aligned} \frac{\partial\psi}{\partial y_{ij}} = & \beta\alpha\epsilon_{ij} - \frac{1}{2}(2\alpha - 1) \ln(x_i x_j) \\ & + \alpha \ln y_{ij} - \frac{1}{2}\beta(\mu_i + \mu_j) - \beta\lambda = 0. \quad (\text{C.7}) \end{aligned}$$

We find the chemical potential for A and B by putting $i = j = A$ or B in Eq. (C.7).

The equilibrium criterion, $\mu_A = \mu_B$, yields, without determining λ ,

$$\begin{aligned} \beta\Delta\mu^0 = & \ln \frac{x_B}{x_A} + \alpha \ln \frac{y_{BB}}{x_B^2} \frac{x_A^2}{y_{AA}} \\ = & \left(1 - \frac{z}{2} \right) \ln \frac{x}{1-x} + \frac{z}{2} \ln \frac{\zeta - 1 + 2x}{\zeta + 1 - 2x}, \quad (\text{C.8}) \end{aligned}$$

where

$$\zeta = [4(\eta^2 - 1)x(1-x) + 1]^{\frac{1}{2}}.$$

The improved result, Eq. (C.8), should take the place of the mean-field result given by Eq. (6).

References

- Akahama, Y., Utsumi, W., Endo, S., Kikegawa, T., Iwasaki, H., Shimomura, O., Yagi, T. & Akimoto, S. (1987), ‘Melting curve of black phosphorous’, *Physics Letters A* **122**(2), 129–131.
URL: <https://www.sciencedirect.com/science/article/pii/0375960187907900>
- Angell, C. A. (2004), ‘Amorphous water’, *Annual Review of Physical Chemistry* **55**(1), 559–583. PMID: 15117262.
URL: <https://doi.org/10.1146/annurev.physchem.55.091602.094156>
- Angell, C. A. (2008), ‘Insights into phases of liquid water from study of its unusual glass-forming properties’, *Science* **319**(5863), 582–587.
URL: <https://www.science.org/doi/abs/10.1126/science.1131939>
- Anisimov, M. A., Duška, M., Caupin, F., Amrhein, L. E., Rosenbaum, A. & Sadus, R. J. (2018), ‘Thermodynamics of fluid polyamorphism’, *Phys. Rev. X* **8**, 011004.
URL: <https://link.aps.org/doi/10.1103/PhysRevX.8.011004>
- Beye, M., Sorgenfrei, F., Schlotter, W. F., Wurth, W. & Föhlisch, A. (2010), ‘The liquid-liquid phase transition in silicon revealed by snapshots of valence electrons’, *Proceedings of the National Academy of Sciences* **107**(39), 16772–16776.
URL: <https://www.pnas.org/content/107/39/16772>
- Bonev, S. A., Schwegler, E., Ogitsu, T. & Galli, G. (2004), ‘A quantum fluid of metallic hydrogen suggested by first-principles calculations’, *Nature* **431**, 669–672.
URL: <https://doi.org/10.1038/nature02968>
- Bragg, W. L. & Williams, E. J. (1934), ‘The effect of thermal agitation on atomic arrangement in alloys’, *Proc. R. Soc. Lond. A* **145**, 699–730.
URL: <http://doi.org/10.1098/rspa.1934.0132>
- Cadien, A., Hu, Q. Y., Meng, Y., Cheng, Y. Q., Chen, M. W., Shu, J. F., Mao, H. K. & Sheng, H. W. (2013), ‘First-order liquid–liquid phase transition in cerium’, *Phys. Rev. Lett.* **110**, 125503.
URL: <https://link.aps.org/doi/10.1103/PhysRevLett.110.125503>
- Dantus, M. & Zewail, A. (2004), ‘Introduction: femtochemistry’, *Chemical Reviews* **104**(4), 1717–1718.
URL: <https://doi.org/10.1021/cr020690k>
- Deemyad, S. & Silvera, I. F. (2008), ‘Melting line of hydrogen at high pressures’, *Phys. Rev. Lett.* **100**, 155701.

- URL:** <https://link.aps.org/doi/10.1103/PhysRevLett.100.155701>
- Eggert, J. H., Weck, G., Loubeyre, P. & Mezouar, M. (2002), ‘Quantitative structure factor and density measurements of high-pressure fluids in diamond anvil cells by x-ray diffraction: Argon and water’, *Phys. Rev. B* **65**, 174105.
- URL:** <https://link.aps.org/doi/10.1103/PhysRevB.65.174105>
- Franzese, G., Marqués, M. I. & Eugene Stanley, H. (2003), ‘Intramolecular coupling as a mechanism for a liquid–liquid phase transition’, *Phys. Rev. E* **67**, 011103.
- URL:** <https://link.aps.org/doi/10.1103/PhysRevE.67.011103>
- Franzese, G. & Stanley, H. E. (2002), ‘Liquid–liquid critical point in a hamiltonian model for water: analytic solution’, *Journal of Physics: Condensed Matter* **14**(9), 2201.
- URL:** <http://stacks.iop.org/0953-8984/14/i=9/a=309>
- Franzese, G. & Stanley, H. E. (2007), ‘The wisdom line of supercooled water’, *Journal of Physics: Condensed Matter* **19**(20), 205126.
- URL:** <https://doi.org/10.1088/0953-8984/19/20/205126>
- Fuchizaki, K. (2013), ‘Melting behavior of SnI₄ reexamined’, *The Journal of Chemical Physics* **139**(24), 244503.
- URL:** <http://scitation.aip.org/content/aip/journal/jcp/139/24/10.1063/1.4851396>
- Fuchizaki, K. (2016), ‘Second critical phenomena expected in tin tetraiodide’, *Journal of the Crystallographic Society of Japan* **58**(1), 42–47.
- URL:** <https://doi.org/10.5940/jcrsj.58.42>
- Fuchizaki, K., Fujii, Y., Ohishi, Y., Ohmura, A., Hamaya, N., Katayama, Y. & Okada, T. (2004), ‘Determination of low-pressure crystalline–liquid phase boundary of SnI₄’, *The Journal of Chemical Physics* **120**(23), 11196–11199.
- URL:** <http://scitation.aip.org/content/aip/journal/jcp/120/23/10.1063/1.1751397>
- Fuchizaki, K., Hamaya, N., Hase, T. & Katayama, Y. (2011), ‘Communication: Probable scenario of the liquid–liquid phase transition of SnI₄’, *The Journal of Chemical Physics* **135**(9), 091101.
- URL:** <http://scitation.aip.org/content/aip/journal/jcp/135/9/10.1063/1.3637038>
- Fuchizaki, K., Hamaya, N. & Katayama, Y. (2013), ‘Characteristic densities of low- and high-pressure liquid SnI₄’, *Journal of the Physical Society of Japan* **82**(3), 033003.
- URL:** <http://dx.doi.org/10.7566/JPSJ.82.033003>
- Fuchizaki, K., Hase, T., Yamada, A., Hamaya, N., Katayama, Y. & Funakoshi, K. (2009), ‘Polyamorphism in tin tetraiodide’, *The Journal of Chemical Physics* **130**(12), 121101.
- URL:** <http://scitation.aip.org/content/aip/journal/jcp/130/12/10.1063/1.3109691>
- Fuchizaki, K., Kohara, S., Ohishi, Y. & Hamaya, N. (2007), ‘Synchrotron x-ray studies of molecular liquid SnI₄’, *The Journal of Chemical Physics* **127**(6), 064504.
- URL:** <http://scitation.aip.org/content/aip/journal/jcp/127/6/10.1063/1.2754265>
- Fuchizaki, K., Ohmura, A., Naruta, H. & Nishioka, T. (2021), ‘The microscopic transition process from high-density to low-density amorphous state of SnI₄’, *Journal of Physics: Condensed Matter* **33**(36), 365401.
- URL:** <https://doi.org/10.1088/1361-648x/ac0dd7>
- Fuchizaki, K., Sakagami, T. & Iwayama, H. (2019), ‘Pressure-induced local symmetry breaking upon liquid–liquid transition of GeI₄ and SnI₄’, *The Journal of Chemical Physics* **150**(11), 114501.
- URL:** <https://doi.org/10.1063/1.5061714>
- Fuchizaki, K., Sugiyama, S. & Fujii, Y. (2000), ‘Search for precursor of pressure-induced amorphization of molecular crystal sni₄: Thermodynamic stability of low-pressure crystalline phase’, *The Journal of Chemical Physics* **112**(23), 10379–10390.
- URL:** <http://scitation.aip.org/content/aip/journal/jcp/112/23/10.1063/1.481675>
- Fujii, Y., Kowaka, M. & Onodera, A. (1985), ‘The pressure-induced metallic amorphous state of SnI₄. I. A novel crystal-to-amorphous transition studied by x-ray scattering’, *Journal of Physics C: Solid State Physics* **18**(4), 789.
- URL:** <http://stacks.iop.org/0022-3719/18/i=4/a=010>
- Gallo, P., Amann-Winkel, K., Angell, C. A., Anisimov, M. A., Caupin, F., Chakravarty, C., Lascaris, E., Loerting, T., Panagiotopoulos, A. Z., Russo, J., Sellberg, J. A., Stanley, H. E., Tanaka, H., Vega, C., Xu, L. & Pettersson, L. G. M. (2016), ‘Water: A tale of two liquids’, *Chemical Reviews* **116**(13), 7463–7500.
- URL:** <https://doi.org/10.1021/acs.chemrev.5b00750>
- Gereben, O. & Pusztai, L. (2012), ‘RMC_POT: A computer code for reverse monte carlo modeling the structure of disordered systems containing molecules of arbitrary complexity’, *Journal of*

- Computational Chemistry* **33**(29), 2285–2291.
URL: <http://dx.doi.org/10.1002/jcc.23058>
- Greaves, G. N., Wilding, M. C., Fearn, S., Langstaff, D., Kargl, F., Cox, S., Van, Q. V., Majrus, O., Benmore, C. J., Weber, R., Martin, C. M. & Hennet, L. (2008), ‘Detection of first-order liquid/liquid phase transitions in yttrium oxide-aluminum oxide melts’, *Science* **322**(5901), 566–570.
URL: <https://www.science.org/doi/abs/10.1126/science.1160766>
- Hamaya, N., Sato, K., Usui-Watanabe, K., Fuchizaki, K., Fujii, Y. & Ohishi, Y. (1997), ‘Amorphization and molecular dissociation of SnI₄ at high pressure’, *Phys. Rev. Lett.* **79**, 4597–4600.
URL: <http://link.aps.org/doi/10.1103/PhysRevLett.79.4597>
- Henry, L., Mezouar, M., Garbarino, G., Sifré, D., Weck, G. & Datchi, F. (2020), ‘Liquid–liquid transition and critical point in sulfur’, *Nature* **584**, 382–386.
URL: <https://doi.org/10.1038/s41586-020-2593-1>
- Hohenberg, P. C. & Halperin, B. I. (1977), ‘Theory of dynamic critical phenomena’, *Rev. Mod. Phys.* **49**, 435–479.
URL: <http://link.aps.org/doi/10.1103/RevModPhys.49.435>
- Hohenberg, P. & Krekhov, A. (2015), ‘An introduction to the Ginzburg-Landau theory of phase transitions and nonequilibrium patterns’, *Physics Reports* **572**, 1–42. An introduction to the GinzburgLandau theory of phase transitions and nonequilibrium patterns.
URL: <https://www.sciencedirect.com/science/article/pii/S0370157315000514>
- Holten, V. & Anisimov, M. A. (2012), ‘Entropy-driven liquid–liquid separation in supercooled water’, *Scientific Reports* **2**, 713.
URL: <https://doi.org/10.1038/srep00713>
- Holten, V., Bertrand, C. E., Anisimov, M. A. & Sengers, J. V. (2012), ‘Thermodynamics of supercooled water’, *The Journal of Chemical Physics* **136**(9), 094507.
URL: <https://doi.org/10.1063/1.3690497>
- Katayama, Y., Inamura, Y., Mizutani, T., Yamakata, M., Utsumi, W. & Shimomura, O. (2004), ‘Macroscopic separation of dense fluid phase and liquid phase of phosphorus’, *Science* **306**(5697), 848–851.
URL: <https://www.science.org/doi/abs/10.1126/science.1102735>
- Katayama, Y., Mizutani, T., Utsumi, W., Shimomura, O., Yamakata, M. & Funakoshi, K.-i. (2000), ‘A first-order liquid–liquid phase transition in phosphorus’, *Nature* **403**, 170–173.
URL: <http://dx.doi.org/10.1038/35003143>
- Kikuchi, R. (1951), ‘A theory of cooperative phenomena’, *Phys. Rev.* **81**, 988–1003.
URL: <https://link.aps.org/doi/10.1103/PhysRev.81.988>
- Kresse, G. & Hafner, J. (1994), ‘Ab initio molecular-dynamics simulation of the liquid-metal–amorphous-semiconductor transition in germanium’, *Phys. Rev. B* **49**, 14251–14269.
URL: <https://link.aps.org/doi/10.1103/PhysRevB.49.14251>
- Lee, B. & Lee, G. W. (2016), ‘A liquid-liquid transition can exist in monatomic transition metals with a positive melting slope’, *Scientific Reports* **6**, 35564.
URL: <http://dx.doi.org/10.1038/srep35564>
- McGreevy, R. L. (2001), ‘Reverse monte carlo modelling’, *Journal of Physics: Condensed Matter* **13**(46), R877.
URL: <http://stacks.iop.org/0953-8984/13/i=46/a=201>
- McMillan, P. F., Wilson, M., Daisenberger, D. & Machon, D. (2005), ‘A density-driven phase transition between semiconducting and metallic polyamorphs of silicon’, *Nature Materials* **4**, 680–684.
URL: <https://doi.org/10.1038/nmat1458>
- McMillan, P. F., Wilson, M. & Wilding, M. C. (2003), ‘Polyamorphism in aluminate liquids’, *Journal of Physics: Condensed Matter* **15**(36), 6105–6121.
URL: <https://doi.org/10.1088/0953-8984/15/36/303>
- McMillan, P. F., Wilson, M., Wilding, M. C., Daisenberger, D., Mezouar, M. & Greaves, G. N. (2007), ‘Polyamorphism and liquid–liquid phase transitions: challenges for experiment and theory’, *Journal of Physics: Condensed Matter* **19**(41), 415101.
URL: <https://doi.org/10.1088/0953-8984/19/41/415101>
- Menelle, A., Bellissent, R. & Flank, A. M. (1987), ‘A neutron scattering study of supercooled liquid tellurium’, *Europhysics Letters (EPL)* **4**(6), 705–708.
URL: <https://doi.org/10.1209/0295-5075/4/6/011>
- Mishima, O., Calvert, L. D. & Whalley, E. (1984), ‘“melting ice” i at 77 k and 10 kbar: a new method of making amorphous solids’, *Nature* **310**, 393–395.
URL: <http://dx.doi.org/10.1038/310393a0>
- Mishima, O., Calvert, L. D. & Whalley, E. (1985), ‘An apparently first-order transition between two amorphous phases of ice induced by pressure’, *Nature*

- ture **314**, 76–78.
URL: <http://dx.doi.org/10.1038/314076a0>
- Mishima, O. & Stanley, H. E. (1998), ‘The relationship between liquid, supercooled and glassy water’, *Nature* **396**, 329–335.
URL: <http://dx.doi.org/10.1038/24540>
- Mituś, A. & Patashinski, A. (1982), ‘The theory of crystal ordering’, *Physics Letters A* **87**(4), 179–182.
URL: <https://www.sciencedirect.com/science/article/pii/0375960182901062>
- Patashinski, A. Z. & Ratner, M. A. (1997), ‘Inherent amorphous structures and statistical mechanics of melting’, *The Journal of Chemical Physics* **106**(17), 7249–7256.
URL: <https://doi.org/10.1063/1.473685>
- Ponyatovsky, E. G. (2003), ‘A thermodynamic approach to t - p phase diagrams of substances in liquid and amorphous states’, *Journal of Physics: Condensed Matter* **15**(36), 6123.
URL: <http://stacks.iop.org/0953-8984/15/i=36/a=304>
- Poole, P. H., Sciortino, F., Essmann, U. & Stanley, H. E. (1992), ‘Phase behaviour of metastable water’, *Nature* **360**, 324–328.
URL: <http://dx.doi.org/10.1038/360324a0>
- Rapoport, E. (1967), ‘Model for melting-curve maxima at high pressure’, *The Journal of Chemical Physics* **46**(8), 2891–2895.
URL: <http://scitation.aip.org/content/aip/journal/jcp/46/8/10.1063/1.1841150>
- Sakagami, T., Fuchizaki, K. & Ohara, K. (2016), ‘A new approach for estimating the density of liquids’, *Journal of Physics: Condensed Matter* **28**(39), 395101.
URL: <http://stacks.iop.org/0953-8984/28/i=39/a=395101>
- Sastry, S., Debenedetti, P. G., Sciortino, F. & Stanley, H. E. (1996), ‘Singularity-free interpretation of the thermodynamics of supercooled water’, *Phys. Rev. E* **53**, 6144–6154.
URL: <https://link.aps.org/doi/10.1103/PhysRevE.53.6144>
- Sauer, G. E. & Borst, L. B. (1967), ‘Lambda transition in liquid sulfur’, *Science* **158**(3808), 1567–1569.
URL: <https://www.science.org/doi/abs/10.1126/science.158.3808.1567>
- Son, L., Rusakov, G., Patashinski, A. & Ratner, M. (1998), ‘Modeling melting in binary systems’, *Physica A: Statistical Mechanics and its Applications* **248**(3), 305–322.
URL: <https://www.sciencedirect.com/science/article/pii/S0378437197005323>
- Speedy, R. J. (1982), ‘Stability-limit conjecture. An interpretation of the properties of water’, *The Journal of Physical Chemistry* **86**(6), 982–991.
URL: <https://doi.org/10.1021/j100395a030>
- Steinhardt, P. J., Nelson, D. R. & Ronchetti, M. (1983), ‘Bond-orientational order in liquids and glasses’, *Phys. Rev. B* **28**, 784–805.
URL: <https://link.aps.org/doi/10.1103/PhysRevB.28.784>
- Stokely, K., Mazza, M. G., Stanley, H. E. & Franzese, G. (2010), ‘Effect of hydrogen bond cooperativity on the behavior of water’, *Proceedings of the National Academy of Sciences* **107**(4), 1301–1306.
URL: <http://www.pnas.org/content/107/4/1301>
- Tanaka, H. (2000), ‘General view of a liquid–liquid phase transition’, *Phys. Rev. E* **62**, 6968–6976.
URL: <https://link.aps.org/doi/10.1103/PhysRevE.62.6968>
- Tanaka, H. (2020), ‘Liquidliquid transition and polyamorphism’, *The Journal of Chemical Physics* **153**(13), 130901.
URL: <https://doi.org/10.1063/5.0021045>
- Tsuchiya, Y. (1991), ‘Thermodynamic evidence for a structural transition of liquid te in the supercooled region’, *Journal of Physics: Condensed Matter* **3**(18), 3163–3172.
URL: <https://doi.org/10.1088/0953-8984/3/18/010>
- Wigner, E. & Huntington, H. B. (1935), ‘On the possibility of a metallic modification of hydrogen’, *The Journal of Chemical Physics* **3**(12), 764–770.
URL: <https://doi.org/10.1063/1.1749590>
- Wilson, K. G. (1971a), ‘Renormalization group and critical phenomena. i. renormalization group and the kadanoff scaling picture’, *Phys. Rev. B* **4**, 3174–3183.
URL: <https://link.aps.org/doi/10.1103/PhysRevB.4.3174>
- Wilson, K. G. (1971b), ‘Renormalization group and critical phenomena. ii. phase-space cell analysis of critical behavior’, *Phys. Rev. B* **4**, 3184–3205.
URL: <https://link.aps.org/doi/10.1103/PhysRevB.4.3184>
- Wu, F. Y. (1982), ‘The potts model’, *Rev. Mod. Phys.* **54**, 235–268.
URL: <https://link.aps.org/doi/10.1103/RevModPhys.54.235>
- Yamane, R., Komatsu, K., Gouchi, J., Uwatoko, Y., Machida, S., Hattori, T., Ito, H. & Kagi, H. (2021), ‘Experimental evidence for the existence of a sec-

ond partially-ordered phase of ice vi', *Nature Communications* **12**, 1129.

URL: <https://doi.org/10.1038/s41467-021-21351-9>

Zaghoo, M., Salamat, A. & Silvera, I. F. (2016), 'Evidence of a first-order phase transition to metallic hydrogen', *Phys. Rev. B* **93**, 155128.

URL: <https://link.aps.org/doi/10.1103/PhysRevB.93.155128>

Zhao, G., Wang, H., Hu, D. M., Ding, M. C., Zhao, X. G. & Yan, J. L. (2017), 'Anomalous phase behavior of first-order fluid-liquid phase transition in phosphorus', *The Journal of Chemical Physics* **147**(20), 204501.

URL: <https://doi.org/10.1063/1.4999009>